

Published in final edited form as:

*Invest Ophthalmol Vis Sci.* 2009 September ; 50(9): 4155–4161. doi:10.1167/iov.09-3561.

## Stromal Edema in *Klf4* Conditional Null Mouse Cornea is Associated with Altered Collagen Fibril Organization and Reduced Proteoglycans

Robert D. Young<sup>1</sup>, Shivalingappa K. Swamynathan<sup>2,\*</sup>, Craig Boote<sup>1</sup>, Mary Mann<sup>2</sup>, Andrew J. Quantock<sup>1</sup>, Joram Piatigorsky<sup>3</sup>, James L. Funderburgh<sup>2</sup>, and Keith M. Meek<sup>1,\*</sup>

<sup>1</sup> Structural Biophysics Group, School of Optometry and Vision Sciences, Cardiff University, Cardiff, UK

<sup>2</sup> Department of Ophthalmology, Eye and Ear Institute, University of Pittsburgh School of Medicine, Pittsburgh, PA, USA

<sup>3</sup> Laboratory of Molecular and Developmental Biology, NEI, NIH, Bethesda, MD, USA

### Abstract

**Purpose**—*Klf4*, one of the highly expressed transcription factors in mouse cornea, plays an important role in maturation and maintenance of the ocular surface. Here, the authors examined the structure and proteoglycan composition of the *Klf4* conditional null (*Klf4*CN) corneal stroma, to further characterize the previously reported *Klf4*CN stromal edema.

**Methods**—Collagen fibril spacing and diameter were calculated from scattering intensity profiles from small angle synchrotron X-ray scattering patterns obtained across the cornea along a vertical meridian at 0.5mm intervals. Collagen fibril organization and proteoglycans were visualised by electron microscopy (EM) with or without the cationic dye Cuproline blue. Proteoglycans and glycosaminoglycans were further analyzed by fluorophore-assisted carbohydrate electrophoresis (FACE) and immunoblots. Q-RT-PCR was used to measure the transcript levels.

**Results**—In the central cornea the average collagen interfibrillar Bragg spacing increased from 44.5nm (SD +/-1.8nm) in wild type to 66.5nm (SD +/-2.3nm) in *Klf4*CN, as measured by X-ray scattering and confirmed by EM. Mean collagen fibril diameter increased from 32nm (SD +/-0.4nm) in wild type to 42.3nm (SD +/-4.8nm) in *Klf4*CN corneal stroma. Downregulation of proteoglycans detected by EM in the *Klf4*CN stroma was confirmed by FACE and immunoblots. Q-RT-PCR showed that while the *Klf4*CN corneal proteoglycan transcript levels remained unchanged, matrix metalloproteinase (MMP) transcript levels were significantly upregulated.

**Conclusions**—The *Klf4*CN corneal stromal edema is characterized by increased collagen interfibrillar spacing and increased diameter of individual fibrils. The stroma also exhibits reduced interfibrillar proteoglycans throughout the corneal stroma, which is possibly caused by increased expression of MMPs.

\*Corresponding authors: 1. Keith M. Meek, Professor and Head, Structural Biophysics Group, School of Optometry and Vision Sciences, Cardiff University, Maindy Road, Cardiff, UK CF24 4LU. 2. Shivalingappa K. Swamynathan, Assistant Professor, Department of Cell Biology and Physiology, and Department of Ophthalmology, University of Pittsburgh School of Medicine, Eye and Ear Institute, 203 Lothrop Street, Room 1025, Pittsburgh PA-15213, USA.

Presented in part at the annual meeting of the Association for Research in Vision and Ophthalmology, Fort Lauderdale, Florida, April 2008.

## Introduction

The cornea consists of a connective tissue stroma of multiple, superimposed lamellae each formed from collagen fibrils with highly regular structure and orientation. The stroma is covered by a stratified epithelium on its outer boundary and a monolayer of endothelial cells lining the inner surface, both cellular populations fulfilling an important barrier function, which influences movement of fluid into and out of the stroma. Corneal transparency is essential for vision and consequently, tight regulation of molecular interactions governing structural integrity and hydration of matrix components is thought to be important in tissue homeostasis both in development and in the adult. Highly ordered collagen architecture with uniformity of fibril diameter and spacing is central to corneal transparency.<sup>1</sup> Collagen fibril diameter may be controlled during fibrillogenesis in the embryo by interaction of different collagen types to form hybrid fibrils.<sup>2-5</sup> Proper hydration of interfibrillar proteoglycans (PGs) appears to be equally important in maintaining appropriate fibril diameter and spacing consistent with optimal light transmission. Overhydration (edema) of stroma is a consequence of impaired function of epithelial or endothelial limiting cell layers, and can occur in a range of corneal dystrophies and pathological conditions, leading to disruption of the ordered ultrastructure, clouding or opacity of the tissue and accompanying loss of vision.<sup>6,7</sup>

Maturation of the fully-functional transparent cornea is driven by complex signalling interactions as well as extrinsic environmental stimuli during development. In rodents, important developmental events take place in association with eyelid opening.<sup>8</sup> To identify changes in gene expression during post natal maturation of the mouse cornea, serial analysis of gene expression was recently employed.<sup>9</sup> Transcription factors associated with barrier function were among the most highly expressed transcription factors in the maturing as well as adult mouse cornea. Foremost amongst these was KLF4, a member of the Krüppel-like transcription factor (KLF) family of zinc finger-containing proteins previously identified as an important regulator of epithelial differentiation in skin, lung and gastrointestinal tract.<sup>10-13</sup> *Klf4* null mice do not survive beyond 15 hours postpartum owing to loss of fluid directly attributable to increased epithelial permeability.<sup>13</sup> The lethal effect of *Klf4* deletion made it impossible to investigate its role in the cornea until recently, following the successful production of hybrid mice with conditional deletion of the *Klf4* gene in the developing ocular surface, using Cre-Lox approach.<sup>14</sup> *Klf4*CN mice are viable and express KLF4 normally, except in the ocular tissues of ectodermal origin including cornea, conjunctiva and lens, where the *Klf4* gene is disrupted. *Klf4*CN corneas contain fewer epithelial cell layers with vacuolated cells, swollen endothelium and edematous stroma, compared to wild type corneas.<sup>14</sup>

Corneal stromal edema is considered to result from “malfunctioning of one or both of the limiting cellular layers”,<sup>15</sup> although endothelial abnormality is normally regarded as the primary cause of stromal changes. An understanding of the factors leading to stromal edema remains important from a clinical standpoint, yet structural matrix changes at the molecular and fibrillar levels which underlie the clinical signs of stromal edema have not been clearly characterized. Mice defective for KLF4 expression thus represent an important model for investigations of mechanisms and molecular interactions involved in this process. Here we report the results of a study using X-ray scattering, electron microscopy and PG analysis to define changes in macromolecular composition and organisation associated with *Klf4*CN stromal edema.

## Materials and Methods

### Animals and tissue acquisition

*Klf4*CN mice with selective disruption of the *Klf4* gene in the cornea, conjunctiva, eyelids and lens were generated as described previously.<sup>14</sup> The following breeding scheme was used to

generate the *Klf4* conditional null (*Klf4*CN) and wild type control sibling mice used in our assays: *Klf4<sup>loxP/loxP</sup>, Le-Cre<sup>-/-</sup>* mice were mated with *Klf4<sup>loxP/loxP</sup>* mice to obtain roughly equal proportion of *Klf4<sup>loxP/loxP</sup>, Le-Cre<sup>-/-</sup>* (*Klf4*CN) and *Klf4<sup>loxP/loxP</sup>* (wild type control siblings) offspring as described before.<sup>14,19</sup> The mice studied here were age matched (12 week-old) on a mixed genetic background and maintained in accordance with the guidelines set forth by the Institutional Animal Care and Use Committee and the ARVO Statement for the Use of Animals in Ophthalmic and Vision Research. Eyes were enucleated from mice euthanized by carbon dioxide asphyxiation and the corneas, together with a rim of sclera, were dissected within ten minutes of death and transferred to 4% paraformaldehyde fixative in 0.1M phosphate buffer.

### X-ray scattering

Corneas were transported in fixative to the Synchrotron Radiation Source, Daresbury, UK and small angle X-ray scattering was carried out with a beam approximately 0.5mm square. Corneas were rinsed briefly in buffer and enveloped in plastic film to prevent dehydration, and the beam was passed through full tissue thickness at the centre. Exposures were made along a vertical meridian at 0.5mm intervals using a computer-operated translation stage. Patterns were analyzed to produce scattering intensity plots from which mean centre-to-centre collagen fibril Bragg spacing and fibril diameter were calculated.

### Electron microscopy

After removal from the X-ray beam, some corneas of wild type and *Klf4*CN mice were fixed for electron microscopy by immersion in either: 2.5% glutaraldehyde in 0.1M sodium cacodylate buffer, followed by aqueous 1% osmium tetroxide for routine electron microscopy; or 2.5% glutaraldehyde in 25mM sodium acetate buffer containing 0.1M magnesium chloride and 0.05% cuproinic blue for PG localisation. Specimens were dehydrated in a graded ethanol series and embedded in Araldite CY212 resin. Sections, 90-100nm thick, were cut from the polymerized resin blocks, collected on uncoated copper grids and stained with uranyl acetate and lead citrate, or uranyl acetate alone for examination in a Philips EM 208 electron microscope.

### Statistical analysis

Collagen fibril spacing in the wild type and *Klf4*CN corneal stroma was calculated for mean +/- SD and tested for normality and equal variance prior to analysis by Student's two-sample T test (Minitab Statistical Software, Minitab Ltd, Coventry, UK). Where data were not normally distributed or of unequal variance the Mann-Whitney test was performed.

### Proteoglycan analysis

Total protein was extracted from 2-3 WT or *Klf4*CN corneas in triplicate using 6 M urea with protease inhibitors as described previously<sup>16</sup> and proteoglycans were isolated using NH<sub>2</sub>-ion exchange microcolumn.<sup>17</sup> Triplicate samples containing equal amounts of protein were digested with 100 mU/ml chondroitinase ABC or keratanase (Sigma) in 0.1M ammonium acetate pH 7.4, at 37° for 16h to digest chondroitin sulfate/dermatan sulfate (CS/DS), or keratan sulfate (KS) glycosaminoglycans (GAGs), respectively. The GAG fragments were recovered by passage through a 2 kDa cut off membrane filter and repeated drying before derivatization with 2-aminoacridone and analysis by using Fluorophore Assisted Carbohydrate Electrophoresis (FACE), as previously described.<sup>17</sup> PG core proteins in the digests were identified by immunoblotting using an antibody to keratocan, Kera-C, (provided by Dr. Winston Kao, University of Cincinnati, Cincinnati, OH), a monoclonal antibody to lumican, Lum-1 (from Dr. Bruce Caterson, Cardiff University, Wales, UK), or to decorin (Sigma), as previously described.<sup>18</sup>

## Isolation of total RNA and Q-RT-PCR

Total RNA isolated from the wild type or *Klf4*CN corneas was quantified and the concentration adjusted with RNase-free water to 100 ng/μl. RT-PCR and Quantitative real time RT-PCR (Q-RT-PCR) assays were done using cDNA generated by High Capacity cDNA Archive Kit and total RNA isolated from pooled corneas of 10 wild type or *Klf4*CN mice. The RT-PCR products were separated on a 2% agarose gel using TBE buffer. Q-RT-PCR assays for different transcripts were performed in ABI 7700 thermocycler using 18S rRNA as endogenous control. The results were analyzed using ABI SDS software. In order to distinguish the products originating from the mRNA from those amplified from the contaminating genomic DNA if any, the forward and reverse primers used in RT-PCR were picked from adjacent exons. The sequence of primers used for RT-PCR and Q-RT-PCR is provided in Supplementary Table 1.

## Results

As measured by synchrotron X-ray diffraction, average collagen fibril spacing in wild type corneas increased from the corneal centre towards the periphery (Fig. 1). *Klf4*CN mouse corneas also exhibited a centre-to-periphery increase in fibril spacing (Fig. 1), but with the spacing in these animals always exceeding that recorded in wild types. Average collagen interfibrillar Bragg spacing in the central cornea increased by about 50%, from 44.5nm (SD +/- 1.8nm) in the wild type (n = 5) to 66.5nm (SD +/- 2.3nm) in the *Klf4*CN stroma (n = 8) (Fig. 1, Table 1). A similar proportional increase was observed in the periphery of the cornea, with the interfibrillar Bragg spacing measuring 65.8nm (SD +/- 11.9nm) in the wild type and 88.7nm (SD +/- 14.5nm) in the *Klf4*CN corneas (Fig. 1, Table 1). These studies also revealed that the average diameter of individual collagen fibrils increased by about 32%, from 32nm (SD +/- 0.4nm) in wild type to 42.3nm (SD +/- 4.8nm) in the *Klf4*CN corneas (Table 1).

Consistent with the X-ray scattering data, electron microscopy also illustrated increased collagen fibril diameter and spacing throughout the depth of the central *Klf4*CN cornea (Fig. 2E-H), compared to the wild type (Fig. 2A-D). Even though the increased collagen fibril spacing and diameter were both evident throughout the *Klf4*CN cornea (compare Fig 2B-D with Fig. 2 F-H), this effect was much more striking in the posterior stroma (compare Fig. 2D with 2H), than the middle or anterior stroma. Electron microscopy also revealed that the *Klf4*CN subepithelial stroma was disrupted with randomly organized collagen fibrils, unlike the regular organization of subepithelial extracellular matrix in the wild type (compare Fig. 2E with Fig. 2A).

Electron microscopy of corneal specimens fixed in the presence of cuproinic blue showed PGs as electron-dense filaments associated with collagen fibrils. PGs appeared considerably reduced in size and abundance in the *Klf4*CN (Fig. 3 G-L) compared to wild type (Fig. 3 A-F) cornea, in both longitudinal (Fig. 3A, C, E, G, I and K) and transverse sections (Fig. 3 B, D, F, H, J and L). This reduction in PGs was observed in the anterior (Fig. 3A, B, G, H), middle (Fig. 3C, D, I, J) and posterior (Fig. 3E, F, K, L) cornea. Consistent with the previous results (Fig. 2), the heightened diameter and spacing of collagen fibrils in *Klf4*CN stroma was also evident at higher magnification in the posterior compared to the central or anterior locations (Fig. 3 K and L compared to Fig. 3 G, H, I and J).

Alterations in stromal proteoglycans of *Klf4*CN corneas were confirmed by biochemical analyses of both core proteins and their GAG chains in total protein extracts of wild type and *Klf4*CN corneas. CS/DS and KS were detected using FACE after digestion with specific endoglycosidases. FACE analysis showed that *Klf4*CN corneas contained about 35% of the wild type levels of CS/DS (both non-sulfated and monosulfated disaccharides), and only 15% of the KS (Fig. 4A and C). Immunoblots with antibodies specific for the PG core proteins, decorin, lumican and keratocan indicated a significant downregulation of all three components

in *Klf4*CN compared to wild type corneas (Fig. 4B). Densitometric scans of these blots showed that decorin, keratocan and lumican were reduced to about 63%, 50% and 6% of the wild type levels respectively, in *Klf4*CN corneas (Fig. 4D). These results imply that lumican and KS GAGs exhibit a greater reduction *pro rata* than decorin and CS/DS GAGs (Fig. 4C). Consistent with the results of cuproinic blue contrast enhanced electron microscopy (Fig. 3), these biochemical analyses provide quantitative estimates of the extent of reduction of GAGs in the *Klf4*CN cornea.

We then compared the expression levels of the transcripts encoding the PGs tested above, in the wild type and *Klf4*CN corneas. Data from the earlier microarray<sup>19</sup> and the current Q-RT-PCR analyses indicated that the transcript levels of decorin, lumican, keratocan and *Chst5* (an enzyme involved in the sulfation of KS chains), do not vary significantly between wild type and *Klf4*CN corneas (Figure 5). To test the possibility that increased degradation of corneal PGs by elevated expression of MMPs may be responsible for the observed reduction in PGs in the *Klf4*CN stroma, we examined the microarray data for the levels of MMPs. We found that MMP2 and MMP9 known to play an active role in corneal extracellular matrix rearrangement during wound healing<sup>20</sup>, and MMP3 as well as MMP13 are indeed upregulated in the *Klf4*CN compared to the WT cornea, by 1.76, 3.5, 2.9 and 4.3-fold, respectively<sup>19</sup>. The upregulation of MMP-2, -3, and -9 expression indicated by microarray analysis was confirmed by RT-PCR (Figure 6).

## Discussion

Maintenance of precise spacing between collagen fibrils with highly regular diameter is considered to be critically important for the transparency of the corneal stroma.<sup>1</sup> Fibril diameter and spacing are influenced by several interacting factors, including the collagen-type composition of the fibrils,<sup>2,3</sup> nature and abundance of the PGs that interact with the fibrils<sup>21-23</sup> and the level of stromal hydration.<sup>24</sup> In this study, we have employed X-ray fiber diffraction to measure the collagen fibril spacing and diameter in wild type and *Klf4*CN mouse corneas, which develop significant stromal edema.<sup>14</sup> Use of an X-ray beam focused to 0.5mm has permitted collection of data from multiple sites across mouse cornea, showing that average interfibrillar spacing of collagen fibrils is higher in the corneal periphery, as previously described in human cornea.<sup>25</sup> Moreover, *Klf4*CN corneas demonstrated significantly increased collagen interfibrillar spacing across the cornea compared to wild type. The collagen fibrils were spread wider apart at all depths in the *Klf4*CN corneal stroma, but with especially increased spacing in posterior regions.

Factors regulating collagen fibril spacing are not fully understood, but evidence suggests that interfibrillar PGs, consisting of a core protein and attached GAG chains, fulfil an important role. Stromal PGs are members of the small leucine-rich proteoglycan (SLRP) family which includes three KS-linked proteins lumican,<sup>26</sup> keratocan<sup>27,28</sup> and osteoglycin,<sup>29</sup> and the CS/DS proteoglycan decorin<sup>30</sup> PGs interact with collagen fibrils at specific sites via their core protein domains,<sup>31</sup> with the sulphated, highly-hydrophilic GAG chains extending into the interfibrillar space where they bind water and thus influence stromal hydration.<sup>32</sup> We found that GAGs, visualized by electron microscopy using cuproinic blue, were markedly reduced in the edematous *Klf4*CN corneal stroma. Biochemical analysis confirmed this reduction using FACE which revealed that both KS and CS/DS GAGs were significantly reduced. The presence of reduced GAGs initially seems difficult to reconcile with tissue edema and increased water content in the *Klf4*CN stroma. Similar decreases in GAG levels have been reported previously, in response to post-surgical and experimentally-induced corneal edema.<sup>33,34</sup> In other situations however, reduced sulfated KS is associated with a more compact stroma with reduced spacing between collagen fibrils; for example, in the *Chst5* knockout mouse cornea,<sup>35</sup> and also in



corneas from patients with macular corneal dystrophy.<sup>36</sup> It therefore seems more likely that the PG loss in *Klf4*CN corneas is a secondary effect of tissue edema rather than its cause.

PG transcript levels in *Klf4*CN corneas were similar to wild type in spite of a reduction in PG and GAG levels, suggesting increased degradation of these molecules in the mutant. Accordingly, in *Klf4*CN corneas we observed an upregulation in MMPs capable of degrading stromal PGs, and which might also contribute to the thinning of the epithelial basement membrane in *Klf4*CN corneas described previously.<sup>14</sup> The results presented here do not allow us to determine if the increased expression of MMPs is due to activation of their promoter activities, or increased stability of their corresponding transcripts. It is possible that the signals generated in response to the *Klf4*CN corneal epithelial fragility or stromal swelling simulate a corneal wounding response and elicit the observed increase in *Klf4*CN corneal MMP expression.

Upregulation of MMPs appears to be a consistent feature concomitant with edema, reported in diverse tissues, including skin, brain and the vascular system,<sup>37,38</sup> as well as human corneas in pseudophakic eyes.<sup>39</sup> In view of the fact that elevated expression of MMPs is associated with tissue remodeling and wound healing<sup>20</sup>, exploring the role of KLF4 in regulating the expression of MMPs in the cornea may reveal if KLF4 influences corneal wound healing by regulating MMPs. The broad spectrum of known activities of the MMP family indicates that, rather than solely regulating matrix turnover, they potentially control many complex aspects of cell behaviour and homeostasis in the extracellular matrix.<sup>40</sup> Thus, upregulation of MMPs probably has far-reaching consequences in the *Klf4*CN phenotype through additional effects on many non-matrix substrates such as cell receptors, signalling and adhesion molecules.

Besides increased interfibrillar spacing in edematous *Klf4*CN corneas, a surprising finding was the increased diameter of stromal collagen fibrils. This may be directly related to the reduction in the amount of PGs, as stromal PGs are known to bind to fibrillar collagen *in vitro* and influence the lateral association of collagen during fibrillogenesis.<sup>22</sup> KS PG-null mice, deficient in lumican, keratocan or osteoglycin, all to some extent exhibit increased diameters of collagen fibrils in corneal stroma.<sup>41-44</sup> Decorin has also been shown to influence fibril diameter and alignment in studies on skin and tendon.<sup>21-23,45</sup> Consistent with our observation that lumican is almost absent from the *Klf4*CN cornea, increased fibril diameters and disrupted fibril spacing were especially prominent in posterior regions of the stroma, where lumican concentrations are highest.<sup>46</sup> However, unlike in our findings, fibril changes were not uniform in PG knockout mice. Rather, clusters of atypical fibrils appeared, scattered amongst relatively normal fibril populations.<sup>41-44</sup>

Edema in *Klf4*CN corneas is manifest as increased fibril spacing throughout the stroma, presumably the result of water ingress following perturbation of epithelial and/or endothelial barriers. Swamynathan et al<sup>14,19</sup> previously showed downregulation of the epithelial water channel proteins, Aquaporins -3 and -5 in *Klf4*CN corneas, while Aquaporin-1 in endothelium was unaltered, and suggested that disturbance to Aquaporin levels might be the reason for stromal edema. This implies a more important role for epithelium in control of stromal hydration than recognised hitherto. Epithelium is instigative in stromal morphogenesis from an early stage in corneal development.<sup>47</sup> *Klf4* expression was detectable in the developing mouse eye from embryonic day 10,<sup>48</sup> at the threshold of major morphogenetic changes involving tissue compaction, loss of water and increasing transparency.<sup>5,46</sup> Perturbation of *Klf4*-driven epithelial differentiation, dysregulation of water channel components and subsequent MMP overexpression appear to contribute to an altered matrix structure which persists in the adult animal. In summary, the results presented in this report provide quantitative measurements of matrix changes that occur with stromal edema in *Klf4*CN corneas and indicate that an increased expression of MMPs is probably responsible for reduced corneal PGs in

*Klf4*CN. Thus, *Klf4*CN mice represent a useful model for further investigations into the physiological mechanisms underlying stromal edema in the cornea.

## Supplementary Material

Refer to Web version on PubMed Central for supplementary material.

## Acknowledgments

Supported by the Medical Research Council, UK (KMM, AJQ, CB, RDY), Intramural Research Program NEI, NIH (JP) and NEI Career Development Award, 1K22 EY016875-01 (SKS), EY09368 (JF). Keith Meek is a Royal Society-Wolfson Research Merit Award holder. James Funderburgh is a Jules and Doris Stein Research to Prevent Blindness Professor.

## References

1. Maurice DM. The structure and transparency of the cornea. *J Physiol* 1957;136:263–286. [PubMed: 13429485]
2. Birk DE, Fitch JM, Babiarz JP, Linsenmayer TF. Collagen type I and type V are present in the same fibril in the avian corneal stroma. *J Cell Biol* 1988;106:999–1008. [PubMed: 3346334]
3. Birk DE, Fitch JM, Babiarz JP, Doane KJ, Linsenmayer TF. Collagen fibrillogenesis in vitro: interaction of types I and V collagen regulates fibril diameter. *J Cell Sci* 1990;95:649–657. [PubMed: 2384532]
4. Linsenmayer TF, Fitch JM, Gordon MK, Cai CX, Igoe F, Marchant JK, Birk DE. Development and roles of collagenous matrices in the embryonic avian cornea. *Prog Retin Eye Res* 1998;17:231–265. [PubMed: 9695794]
5. Quantock AJ, Young RD. Development of the corneal stroma and the collagen-proteoglycan associations that help define its structure and function. *Dev Dynam* 2008;237:2607–2621. Review
6. Edelhauser HF. The balance between corneal transparency and edema: the Proctor Lecture. *Invest Ophthalmol Vis Sci* 2006;47(5):1754–67. [PubMed: 16638979]
7. Meek KM, Leonard DW, Cannon CJ, Dennis S, Khan S. Transparency, swelling and scarring in the corneal stroma. *Eye* 2003;17(8):927–36. [PubMed: 14631399]
8. Zieske JD. Corneal development associated with eyelid opening. *Int J Dev Biol* 2004;48:903–911. [PubMed: 15558481]
9. Norman B, Davis J, Piatigorsky J. Postnatal gene expression in the normal mouse cornea by SAGE. *Invest Ophthalmol Vis Sci* 2004;45:429–440. [PubMed: 14744882]
10. Garrett-Sinha LA, Eberspaecher H, Seldin MF, de Crombrughe B. A gene for a novel zinc-finger protein expressed in differentiated epithelial cells and transiently in certain mesenchymal cells. *J Biol Chem* 1996;271:31384–31390. [PubMed: 8940147]
11. Shields JM, Christy RJ, Yang VW. Identification and characterization of a gene encoding a gut-enriched Kruppel-like factor expressed during growth arrest. *J Biol Chem* 1996;271:20009–20017. [PubMed: 8702718]
12. Katz JP, Perreault N, Goldstein BG, et al. The zinc-finger transcription factor *Klf4* is required for terminal differentiation of goblet cells in the colon. *Development* 2002;129:2619–2628. [PubMed: 12015290]
13. Segre JA, Bauer C, Fuchs E. *Klf4* is a transcription factor required for establishing the barrier function of the skin. *Nat Genet* 1999;22:356–360. [PubMed: 10431239]
14. Swamynathan SK, Katz JP, Kaestner KH, Ashery-Padan R, Crawford MA, Piatigorsky J. Conditional deletion of the mouse *Klf4* gene results in corneal epithelial fragility, stromal edema and loss of conjunctival goblet cells. *Mol Cell Biol* 2007;27:182–194. [PubMed: 17060454]
15. Dolhman, CH. Physiology of the Cornea: corneal edema. In: Smolin, G.; Thoft, RA., editors. *The Cornea Scientific Foundations and Clinical Practice*. Little, Brown & Co; 1983. p. 3-17.

16. Funderburgh JL, Funderburgh ML, Mann MM, Conrad GW. Arterial lumican. Properties of a corneal-type keratan sulfate proteoglycan from bovine aorta. *J Biol Chem* 1991;266:24773–24777. [PubMed: 1761572]
17. Funderburgh JL, Mann MM, Funderburgh ML. Keratocyte phenotype mediates proteoglycan structure: a role for fibroblasts in corneal fibrosis. *J Biol Chem* 2003;278:45629–45637. [PubMed: 12933807]
18. Funderburgh ML, Mann MM, Funderburgh JL. Keratocyte phenotype is enhanced in the absence of attachment to the substratum. *Mol Vis* 2008;14:308–17. [PubMed: 18334944]
19. Swamynathan SK, Davis J, Piatigorsky J. Identification of candidate Klf4 target genes reveals the molecular basis of the diverse regulatory roles of Klf4 in the mouse cornea. *Invest Ophthalmol Vis Sci* 2008;49:3360–3370. [PubMed: 18469187]
20. Sivak JM, Fini EM. MMPs in the eye: emerging roles for matrix metalloproteinases in ocular physiology. *Progress Retinal Eye Res* 2002;21:1–14.
21. Vogel KG, Trotter JA. The effect of proteoglycans on the morphology of collagen fibrils formed in vitro. *Coll Relat Res* 1987;7:105–14. [PubMed: 3621881]
22. Rada JA, Cornuet PK, Hassell JR. Regulation of corneal collagen fibrillogenesis in vitro by corneal proteoglycan (lumican and decorin) core proteins. *Exp Eye Res* 1993;56:635–48. [PubMed: 8595806]
23. Zhang G, Young BB, Ezura Y, et al. Development of tendon structure and function: regulation of collagen fibrillogenesis. *J Musculoskelet Neuronal Interact* 2005;5:5–21. [PubMed: 15788867]
24. Meek KM, Fullwood NJ, Cooke PH, et al. Synchrotron x-ray diffraction studies of the cornea, with implications for stromal hydration. *Biophys J* 1991;60:467–474. [PubMed: 1912282]
25. Boote C, Dennis S, Newton RH, Puri H, Meek KM. Collagen fibrils appear more closely packed in the prepupillary cornea: optical and biomechanical implications. *Invest Ophthalmol Vis Sci* 2003;44:2941–8. [PubMed: 12824235]
26. Blochberger TC, Vergnes JP, Hempel J, Hassell JR. cDNA to chick lumican (corneal keratan sulfate proteoglycan) reveals homology to the small interstitial proteoglycan gene family and expression in muscle and intestine. *J Biol Chem* 1992;267:347–352. [PubMed: 1370446]
27. Corpuz LM, Funderburgh JL, Funderburgh ML, Bottomley GS, Prakash S, Conrad GW. Molecular cloning and tissue distribution of keratocan. Bovine corneal keratan sulfate proteoglycan 37A. *J Biol Chem* 1996;271:9759–9763. [PubMed: 8621655]
28. Liu CY, Shiraishi A, Kao CW, et al. The cloning of mouse keratocan cDNA and genomic DNA and the characterization of its expression during eye development. *J Biol Chem* 1998;273:22584–22588. [PubMed: 9712886]
29. Funderburgh JL, Corpuz LM, Roth MR, Funderburgh ML, Tasheva ES, Conrad GW. Mimecan, the 25-kDa corneal keratan sulfate proteoglycan, is a product of the gene producing osteoglycin. *J Biol Chem* 1997;272:28089–28095. [PubMed: 9346963]
30. Li W, Vergnes JP, Cornuet PK, Hassell JR. cDNA clone to chick corneal chondroitin dermatan sulfate proteoglycan reveals identity to decorin. *Arch Biochem Biophys* 1992;296:190–197. [PubMed: 1605630]
31. Scott JE, Haigh M. ‘Small’-proteoglycan:collagen interactions: keratan sulphate proteoglycan associates with rabbit corneal collagen fibrils at the ‘a’ and ‘c’ bands. *Biosci Rep* 1985;5:765–774. [PubMed: 2935202]
32. Bettelheim FA, Plessy B. The hydration of proteoglycans of bovine cornea. *Biochim Biophys Acta* 1975;381:203–214. [PubMed: 122899]
33. Anseth A. Studies on corneal polysaccharides. V. Changes in corneal glycosaminoglycans in transient stromal edema. *Exp Eye Res* 1969;8:297–301. [PubMed: 4240715]
34. Kangas TA, Edelhauser HF, Twining SS, O’Brien WJ. Loss of stromal glycosaminoglycans during corneal edema. *Invest Ophthalmol Vis Sci* 1990;31:1994–2002. [PubMed: 2210995]
35. Hayashida Y, Akama TO, Beecher N, et al. Matrix morphogenesis in cornea is mediated by the modification of keratan sulphate by GlcNAc 6-O-sulfotransferase. *Proc Natl Acad Sci USA* 2006;5:13333–13338. [PubMed: 16938851]



36. Quantock AJ, Meek KM, Ridgway AE, Bron AJ, Thonar EJ. Macular corneal dystrophy: reduction in both corneal thickness and collagen interfibrillar spacing. *Curr Eye Res* 1990;9:393–398. [PubMed: 2340750]
37. Järvinen TM, Jeskanen L, Koskenmies S, et al. Matrix metalloproteinases as mediators of tissue injury in different forms of cutaneous lupus erythematosus. *Brit J Dermatol* 2007;157:970–980. [PubMed: 17854363]
38. Von Gertten C, Holmin S, Mathiesen T, Nordqvist AC. Increase in matrix metalloproteinase-9 and tissue inhibitor of metalloproteinase-1 mRNA after cerebral contusion and depolarisation. *2003;73:803–810.*
39. Shoshani Y, Pe'er J, Doviner V, Frucht-Pery J, Solomon A. Increased expression of inflammatory cytokines and matrix metalloproteinases in pseudophakic corneal edema. *Invest Ophthalmol Vis Sci* 2005;46:1940–1947. [PubMed: 15914607]
40. Overall CM. Dilating the degradome: matrix metalloproteinase 2 (MMP-2) cuts to the heart of the matter. *Biochem J* 2004;383:e5–e7. [PubMed: 15508185]
41. Chakravarti S, Magnuson T, Lass JH, Jepsen KJ, LaMantia C, Carroll H. Lumican regulates collagen fibril assembly: skin fragility and corneal opacity in the absence of lumican. *J Cell Biol* 1998;141:1277–86. [PubMed: 9606218]
42. Chakravarti S, Petroll WM, Hassell JR, et al. Corneal opacity in lumican-null mice: Defects in collagen fibril structure and packing in the posterior stroma. *Invest Ophthalmol Vis Sci* 2000;4:3365–3373. [PubMed: 11006226]
43. Liu CY, Birk DE, Hassell JR, Kane B, Kao WW. Keratocan-deficient mice display alterations in corneal structure. *J Biol Chem* 2003;278:21672–21677. [PubMed: 12665512]
44. Tasheva ES, Koester A, Paulsen AQ, et al. Mimecan/osteoglycin-deficient mice have collagen fibril abnormalities. *Mol Vis* 2002;8:407–415. [PubMed: 12432342]
45. Danielson KG, Baribault H, Holmes DF, Graham H, Kadler KE, Iozzo RV. Targeted disruption of decorin leads to abnormal collagen fibril morphology and skin fragility. *J Cell Biol* 1997;136:729–43. [PubMed: 9024701]
46. Chakravarti S, Zhang G, Chervoneva I, Roberts L, Birk DE. Collagen fibril assembly during postnatal development and dysfunctional regulation in the lumican-deficient murine cornea. *Dev Dyn* 2006;235:2493–2506. [PubMed: 16786597]
47. Hay, ED.; Revel, JP. Fine structure of the developing avian cornea. In: Wolsky, A.; Chen, PS., editors. *Monographs in Developmental Biology*. Vol. 1. S Karger; 1969. p. 1-144.
48. Ehlermann J, Pfisterer P, Schorle H. Dynamic expression of Krüppel-like factor 4 (Klf4), a target of transcription factor AP-2 $\alpha$  during murine mid-embryogenesis. *Anat Rec* 2003;677–680.

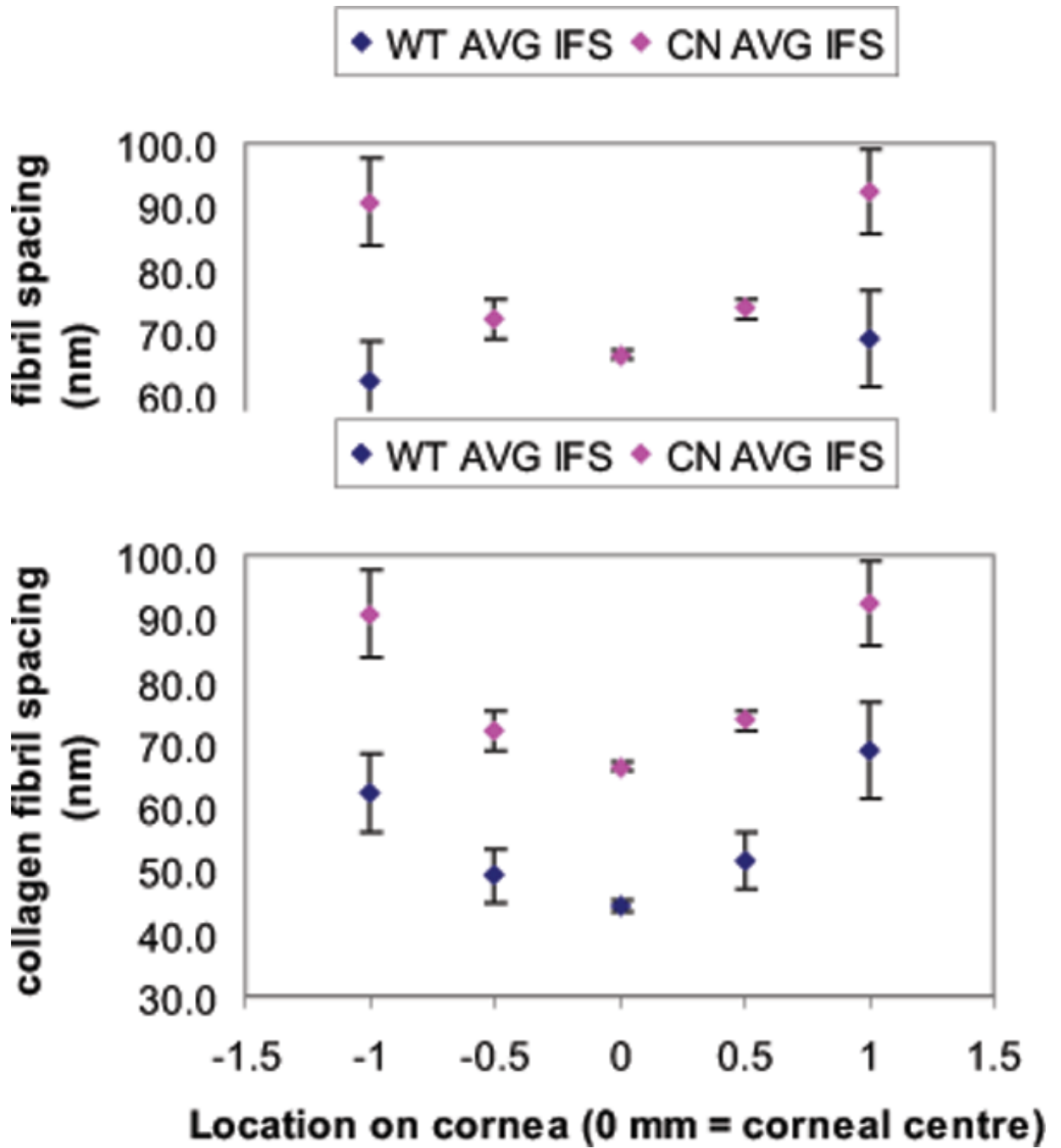


**Figure 1.** Graphical representation of average collagen interfibrillar (Bragg) spacing (y-axis) from X-ray scattering patterns obtained at 5 sites at 0.5 mm intervals (x axis) along a vertical meridian across the cornea in 5 wild type and 8 *Klf4*CN mice. In both wild type and *Klf4*CN stroma, the interfibrillar spacing becomes increasingly greater on moving further towards the periphery from the corneal centre (represented by 0mm). Fibril spacing in the *Klf4*CN mouse cornea exceeds that in wild type across the meridian.

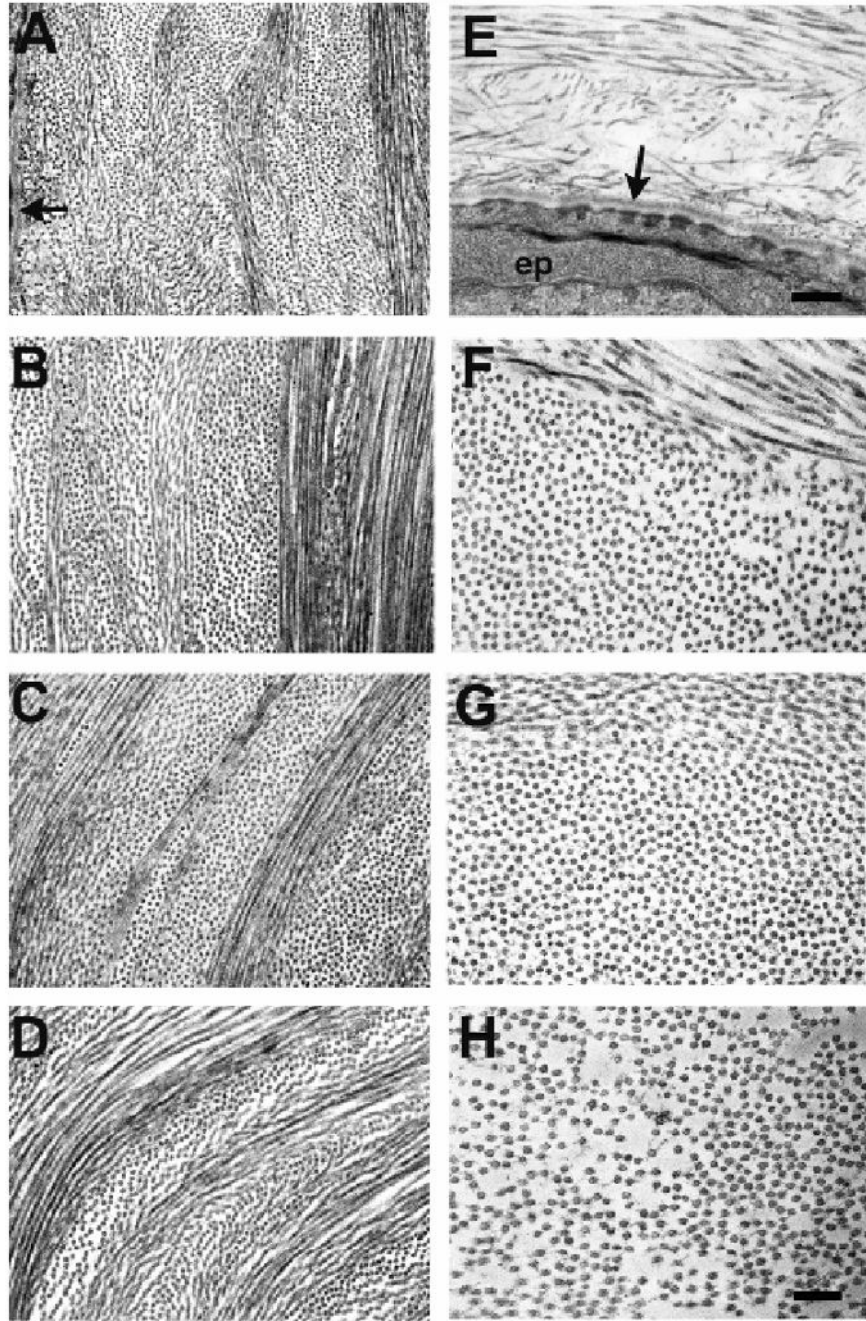


**Figure 2.** Electron micrographs of corneal lamellae in wild type (A-D) and *Klf4CN* corneal stroma (E-H). Subepithelial stroma appears disrupted in mutant cornea (E); arrows indicate basal lamina below epithelium; anterior stroma (B and F); mid stroma (C and G); posterior stroma (D and H). Bar = 480nm (A, E), 300nm (B-D, F-H).



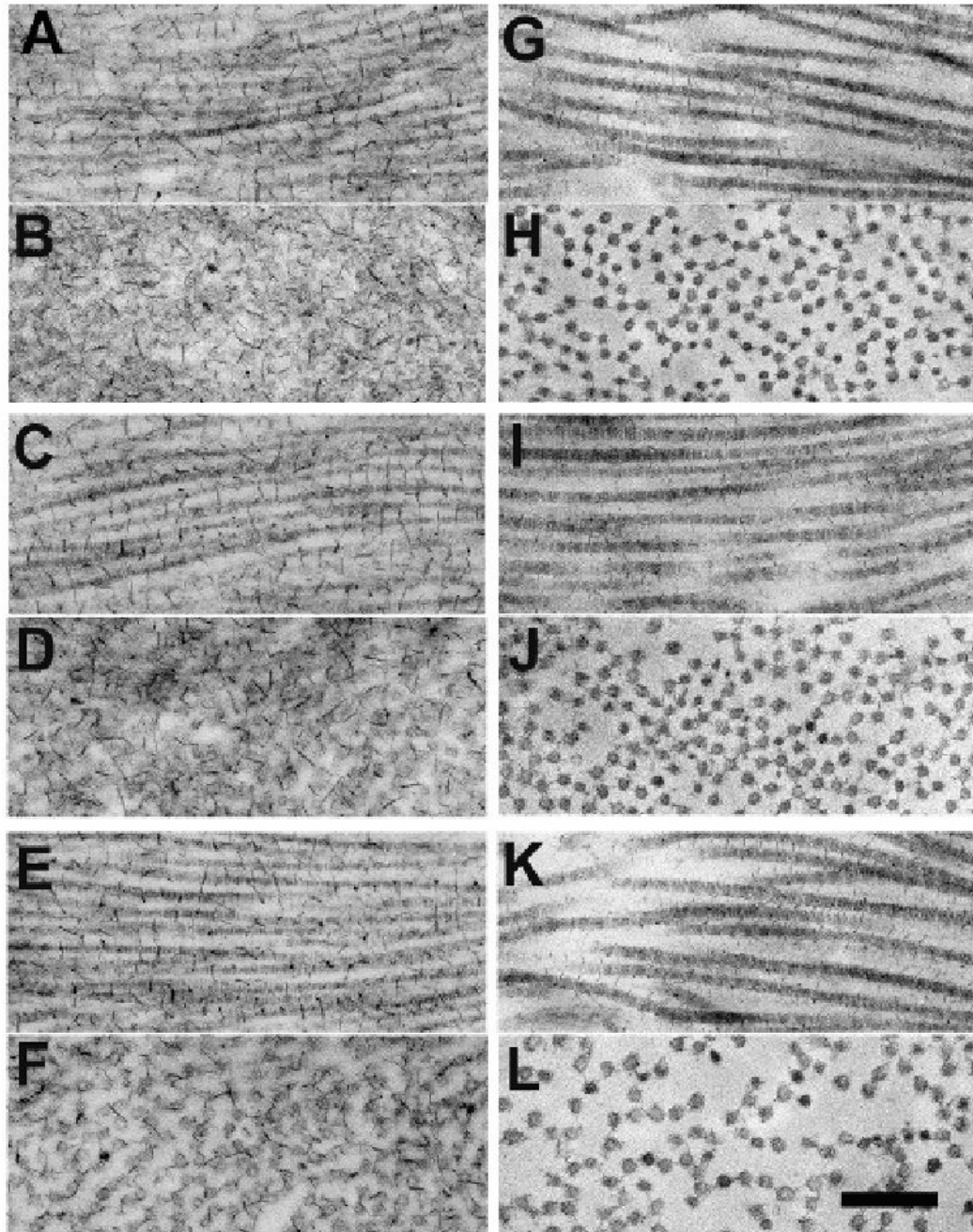
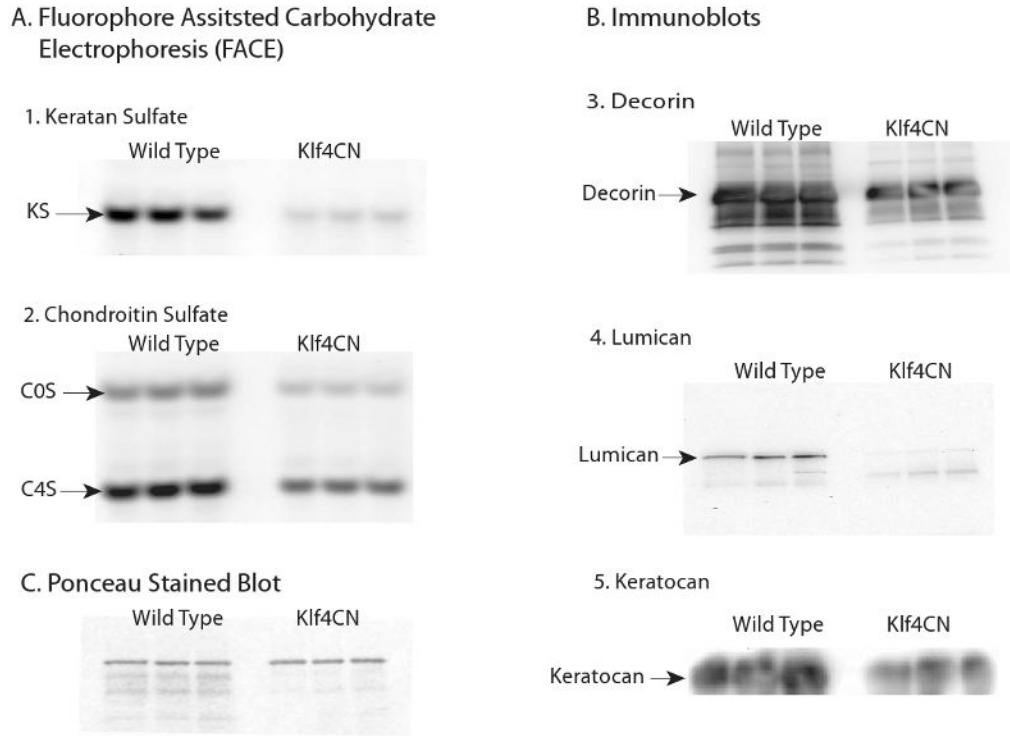


**Figure 3.**

Electron micrographs of cornea in anterior, mid and posterior stroma from wild type (A-F) and *Klf4CN* cornea (G-L), prepared with contrast enhanced fixation of proteoglycans (PGs) using cuproinic blue. Collagen fibrils appear in longitudinal (A,C,E,G,I and K) and transverse (B,D,F,H,J and L) section. PGs are seen as fine filaments decorating collagen fibrils and are more prominent in wild-type than *Klf4CN* mouse cornea, where interfibrillar spacing is also seen to be increased. Bar = 300nm.



D. Quantitative Densitometric Scan of the above blots with error bars

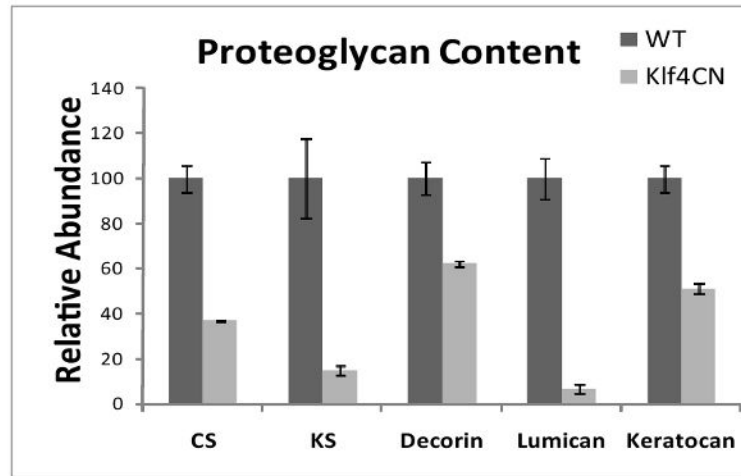


**Figure 4.** Analysis of proteoglycans extracted from wild type and *Klf4CN* mouse corneas.  
 A. Fluorophore-assisted carbohydrate electrophoresis analysis of: (1.) Keratan sulfate-(KS) monosulfated disaccharides generated by keratanase digestion. (2.) Unsulfated (COS) and monosulfated (C4S) CS/DS disaccharides generated by chondroitinase ABC digestion.  
 B. Western blot identification of:  
 3. Decorin core protein  
 4. Lumican core protein  
 5. Keratocan core protein.  
 C. Ponceau stained blot showing equal protein loading.



D. For each of these analyses, quantitative analysis of three replicates from wild type and *Klf4*CN corneal extracts are displayed with standard error. In each case differences were statistically significant ( $p < 0.05$ ).

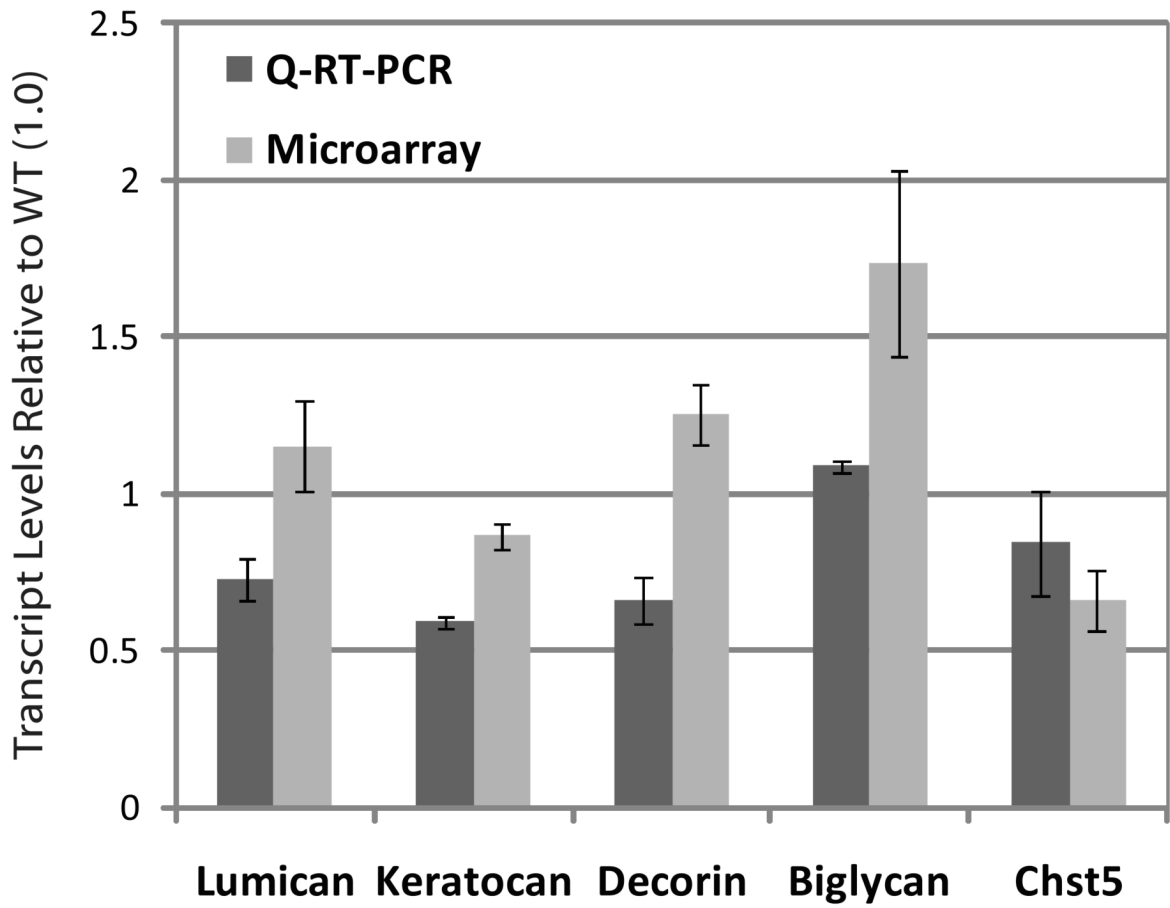


**Figure 5.** Expression of proteoglycan-related transcripts in the *Klf4CN* compared to wild type cornea. Relative expression of different proteoglycan transcripts in the *Klf4CN* compared to wild type corneas, measured by Q-RT-PCR and microarray analyses is depicted. The corresponding values are depicted within the histogram bars.

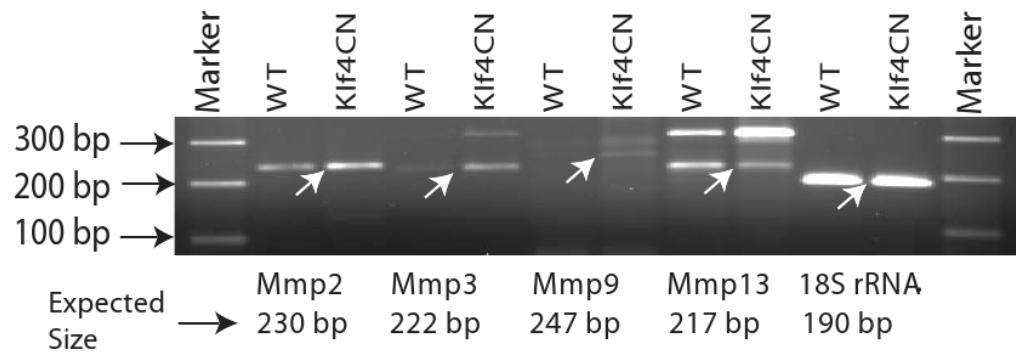


**Figure 6.**

Elevated expression of MMPs in the *Klf4CN* cornea. RT-PCR analysis of expression levels of transcripts encoding MMP2, 3, 9 and 13, in the WT and *Klf4CN* corneas. Expression levels of 18S rRNA transcripts are used as endogenous controls. The expected amplicons are indicated by arrows in the gel picture, with the corresponding expected amplicon sizes indicated below the gel photo for each MMP.

**Table 1**  
 Summary of collagen interfibrillar (Bragg) spacing at corneal centre and periphery and fibril diameter at the corneal centre calculated from X-ray scatter patterns obtained in wild type (n=5) and *Klf4*CN (n=8) mice.

Mouse #	Wild Type			Mouse #	<i>Klf4</i> CN		
	Interfibrillar Bragg Spacing (nm)		Fibril Diameter (nm)		Interfibrillar Bragg Spacing (nm)		Fibril Diameter (nm)
	Centre	Periphery	Centre		Centre	Periphery	Centre
425	44	76.7	32.2	426	65.5	109.4	38.6
425A	42.1	51	31.5	426A	65.5	75.6	37.7
437	45.4	59	31.7	436	64.1	67	38.6
437A	44	79	31.9	424	65.5	92.1	47.3
423	46.8	63.2	32.6	432	65.5	75.6	43.8
				435	70.2	100	51.3
				429	70.2	95.1	40.9
				433	65.5	95.1	40.2
<b>Mean</b>	<b>44.5</b>	<b>65.8</b>	<b>32.0</b>		<b>66.5</b>	<b>88.7</b>	<b>42.3</b>
<b>Standard Deviation</b>	<b>1.8</b>	<b>11.9</b>	<b>0.4</b>		<b>2.3</b>	<b>14.5</b>	<b>4.8</b>
<b>Standard Error</b>	<b>0.8</b>	<b>5.3</b>	<b>0.2</b>		<b>0.8</b>	<b>5.1</b>	<b>1.7</b>